The Plant Cell, Vol. 25: 2986–2997, August 2013, www.plantcell.org

The Clathrin Adaptor Complex AP-2 Mediates Endocytosis of BRASSINOSTEROID INSENSITIVE1 in *Arabidopsis*[W]

Simone Di Rubbo,[a,b] Niloufer G. Irani,[a,b,1] Soo Youn Kim,[c] Zheng-Yi Xu,[c] Astrid Gadeyne,[a,b] Wim Dejonghe,[a,b] Isabelle Vanhoutte,[a,b] Geert Persiau,[a,b] Dominique Eeckhout,[a,b] Sibu Simon,[a,b,2] Kyungyoung Song,[c] Jürgen Kleine-Vehn,[a,b,3] Jiří Friml,[a,b,2] Geert De Jaeger,[a,b] Daniël Van Damme,[a,b] Inhwan Hwang,[c] and Eugenia Russinova[a,b,4]

[a] Department of Plant Systems Biology, VIB, 9052 Ghent, Belgium
[b] Department of Plant Biotechnology and Bioinformatics, Ghent University, 9052 Ghent, Belgium
[c] Division of Molecules and Life Sciences and Center for Plant Intracellular Trafficking, Pohang University of Science and Technology, Pohang 790-784, Korea

Clathrin-mediated endocytosis (CME) regulates many aspects of plant development, including hormone signaling and responses to environmental stresses. Despite the importance of this process, the machinery that regulates CME in plants is largely unknown. In mammals, the heterotetrameric ADAPTOR PROTEIN COMPLEX-2 (AP-2) is required for the formation of clathrin-coated vesicles at the plasma membrane (PM). Although the existence of AP-2 has been predicted in *Arabidopsis thaliana*, the biochemistry and functionality of the complex is still uncharacterized. Here, we identified all the subunits of the *Arabidopsis* AP-2 by tandem affinity purification and found that one of the large AP-2 subunits, AP2A1, localized at the PM and interacted with clathrin. Furthermore, endocytosis of the leucine-rich repeat receptor kinase, BRASSINOSTEROID INSENSITIVE1 (BRI1), was shown to depend on AP-2. Knockdown of the two *Arabidopsis AP2A* genes or overexpression of a dominant-negative version of the medium AP-2 subunit, *AP2M*, impaired BRI1 endocytosis and enhanced the brassinosteroid signaling. Our data reveal that the CME machinery in *Arabidopsis* is evolutionarily conserved and that AP-2 functions in receptor-mediated endocytosis.

INTRODUCTION

Cells need to constantly regulate the turnover and activity of proteins present at their plasma membrane (PM) in response to extracellular and intracellular cues. Endocytosis selectively internalizes integral PM proteins and extracellular macromolecules by forming and budding-off vesicles into the cytoplasm. One of the best described routes for selective internalization in eukaryotic cells uses the scaffolding protein clathrin, hence, its designation as clathrin-mediated endocytosis (CME). CME requires a network of proteins, including clathrin, adaptors, and accessory proteins responsible for selection and recruitment of cargos (Traub, 2009; McMahon and Boucrot, 2011). Clathrin and PM cargo proteins are recruited to form clathrin-coated vesicles at the PM through mediation of the ADAPTOR PROTEIN COMPLEX-2 (AP-2) (Rappoport and Simon, 2009; McMahon and Boucrot, 2011). AP-2 is a heterotetrameric complex consisting of two large subunits (α2 and β2 or AP2A and AP2B), one medium subunit (μ2 or AP2M), and one small subunit (σ2 or AP2S) (Collins at al., 2002; Hirst et al., 2011). AP-2 forms the core hub of the CME because it binds simultaneously to cargo proteins, PM-residing lipids (Krauss et al., 2006), and clathrin. AP-2 recognizes specific endocytic cargo motifs directly, such as dileucine ([GluAsp] xxxLeu[Leu/Ile]) and Tyr (TyrxxΦ, where Φ represents a bulky hydrophobic amino acid) (Kelly et al., 2008; Traub, 2009; Jackson et al., 2010), or interacts with clathrin-associated sorting proteins (such as AP180, epsins, and the epidermal growth factor receptor substrate 15) to recognize the cargos (Traub, 2009; McMahon and Boucrot, 2011). Depletion of AP-2 function in mammalian cells blocks the uptake of transferrin and depletes clathrin from the PM, demonstrating that the complex is essential for endocytosis (Boucrot et al., 2010).

Although in plants CME has been linked to the regulation of auxin transport (Dhonukshe et al., 2007; Robert et al., 2010; Kitakura et al., 2011), brassinosteroid (BR) signaling (Irani et al., 2012), pathogen responses (Sharfman et al., 2011; Adam et al., 2012), nutrient uptake, and toxicity avoidance (Takano et al., 2010; Barberon et al., 2011), the components of its machinery remain largely unknown (Chen et al., 2011). Despite some biochemical evidence for the existence of an AP-2 in plants (Holstein et al., 1994; Robinson et al., 1998; Barth and Holstein, 2004; Happel et al., 2004, Lee et al., 2007), the complex has not been characterized, and no genetic studies supporting its

[1] Current address: Department of Plant Sciences, University of Oxford, South Parks Road, Oxford OX1 3RB, UK.
[2] Current address: Institute of Science and Technology Austria, 3400 Klosterneuburg, Austria.
[3] Current address: Department of Applied Genetics and Cell Biology, University of Natural Resources and Life Sciences (BOKU), 1190 Vienna, Austria.
[4] Address correspondence to eugenia.russinova@psb.vib-ugent.be.
The author responsible for distribution of materials integral to the findings presented in this article in accordance with the policy described in the Instructions for Authors (www.plantcell.org) is: Eugenia Russinova (eugenia.russinova@psb.vib-ugent.be).
[W] Online version contains Web-only data.
www.plantcell.org/cgi/doi/10.1105/tpc.113.114058

role in endocytosis have been reported to date. However, experimental data suggest that the mechanism regulating CME is conserved between plants and mammals. For example, the tomato (*Solanum lycopersicum*) receptor ELICITOR INDUCED XILANASE2 (EIX2) carries a TyrxxF sequence motif required for the interaction with the AP2M subunit of AP-2 in mammals (Bar and Avni, 2009). Additionally, mutations in the similar TyrxxΦ motif in the boron transporter BOR1 inhibit its endocytosis (Takano et al., 2010). Similarly, the vacuolar sorting receptor VSR-PS1 interacts in vitro with AP2M via the same motif (Happel et al., 2004) and the human transferrin receptor can undergo ligand-stimulated endocytosis when expressed in *Arabidopsis thaliana* protoplasts, which is an AP-2–dependent process in mammalian cells (Ortiz-Zapater et al., 2006).

Here, we identified the core AP-2 complex of *Arabidopsis* via tandem affinity purification (TAP) using one of the two putative large AP-2 subunits (AP2A1) as bait. The AP-2 complex was highly similar to its mammalian counterpart and consisted of four subunits (AP2A1, AP1/2B1/2, AP2M, and AP2S), of which AP2A1 localized predominately at the PM and interacted with clathrin and the BR receptor BRASSINOSTEROID INSENSITIVE1 (BRI1). AP-2 knockdown and dominant-negative *Arabidopsis* lines impaired BRI1 endocytosis and enhanced BR signaling. Our results show that AP-2 is an evolutionarily conserved feature of CME and that it contributes to the endocytic regulation of BR signaling in plants.

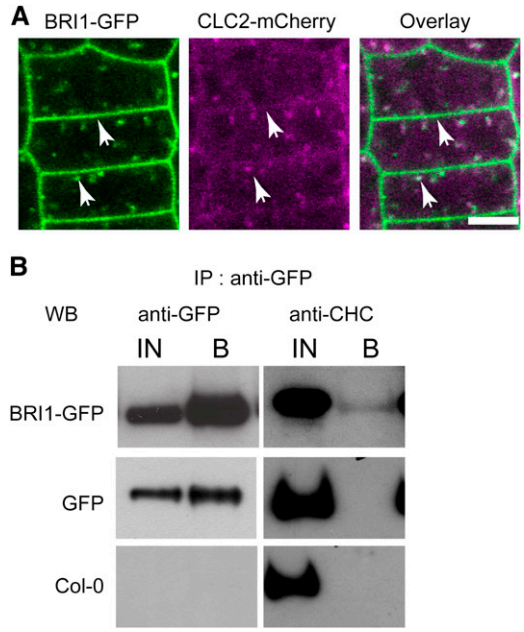

Figure 1. Colocalization and Interaction between BRI1 and Clathrin.

(A) Colocalization of BRI1-GFP with CLC2-mCherry at the PM and in endosomes (arrows) in epidermal cells of the *Arabidopsis* root meristem. Bar = 5 μm.

(B) Coimmunoprecipitation of CHC with BRI1. Total extracts of 7-d-old seedlings expressing *BRI1-GFP*, *GFP*, and the wild type (Col-0) were incubated with agarose-conjugated anti-GFP antibodies and probed with anti-CHC or anti-GFP antibodies. IN is equivalent to 20% of the protein incubated with the beads for immunoprecipitation. IP, immunoprecipitation; WB, protein gel blot; IN, input; B, bound fraction.

RESULTS

BRI1 Colocalizes and Interacts with Clathrin

Previously, we had shown that a clathrin function was required for the internalization of the BR receptor BRI1 (Irani et al., 2012). To corroborate this observation, we performed colocalization experiments in epidermal cells of the *Arabidopsis* root meristem that coexpressed the fusion proteins BRI1–green fluorescent protein (GFP) (Friedrichsen et al., 2000) and CLATHRIN LIGHT CHAIN2 (CLC2)–mCherry (Van Damme et al., 2011). In agreement with the reported CME of the receptor (Irani et al., 2012), BRI1 colocalized with CLC2 at the PM and in CLC2-mCherry–positive endosomes (Figure 1A) that had been found previously to be mainly *trans*-Golgi network (TGN)/early endosome compartments (Ito et al., 2012). Additionally, coimmunoprecipitation experiments with *Arabidopsis* seedlings expressing *BRI1-GFP* probed with anti–clathrin heavy chain (CHC) antibodies (Figure 1B) revealed that clathrin and BRI1 interacted. The occurrence of BRI1 and clathrin together in the endomembrane system supports the CME model for BRI1 internalization (Irani et al., 2012).

Isolation of the *Arabidopsis* AP-2 Complex

Despite the evidence that BRI1 undergoes CME, studies of this mechanism are limited by the poor knowledge of the CME machinery in plants. As clathrin does not bind PM cargos directly, we speculate that, similar to the mammalian CME model (Rappoport and Simon, 2009; McMahon and Boucrot, 2011), the AP-2 complex might mediate this interaction. In support of this hypothesis, AP2A1 (At5g22770), one of the two putative *Arabidopsis* AP-2 large subunits (Bassham et al., 2008), was used to isolate the AP-2 complex from PSB-D *Arabidopsis* cell suspension cultures. In TAP experiments, AP2A1 was fused to a G protein and a streptavidin-binding peptide (GS) tag at its C or N terminus (Bürckstümmer et al., 2006; Van Leene et al., 2008) and was produced under a cauliflower mosaic virus (CaMV) 35S promoter in *Arabidopsis* cell cultures. A complex comprising AP2A1 and five additional proteins was isolated repeatedly and independently of the tag position (Table 1; see Supplemental Figure 1 and Supplemental Table 1 online). Four of the identified proteins, namely, AP1/2B1 (At4g11380), AP1/2B2 (At4g23460), AP2M (At4g46630), and AP2S (At1g47830), had been predicted to be part of the AP-2 complex in *Arabidopsis* inferred from homology to their mammalian counterparts (Bassham et al., 2008). Additionally, in two of the four purifications, a putative AP2A1 binding protein (At5g65960) was identified as well (Table 1; see Supplemental Figure 1 and Supplemental Table 1 online).

The interactions found via the TAP technology were reconfirmed by bimolecular fluorescent complementation (BiFC). The AP-2 subunits were fused to the C-terminal or N-terminal fragments of the GFP (designated cGFP and nGFP, respectively) and produced transiently in the leaf epidermis of *Nicotiana*

Table 1. The AP-2 Complex of *Arabidopsis* Identified by TAP Experiments

AT No.	Name	Found in TAP-AP2A1 (Two TAPs)	Found in AP2A1-TAP (Two TAPs)	Found in Four TAPs	Protein Score	Expected	Best Ion Score	Expected
At5G22770	α-Adaptin (AP2A1)	2/2	2/2	4	1590	3.30E-155	155	6.7E-15
At1G47830	Clathrin coat assembly protein, putative (AP2S)	2/2	2/2	4	542	2.10E-50	156	3.2E-15
At4G11380	β-Adaptin, putative (AP1/2B1)	2/2	2/2	4	1300	3.30E-126	153	5.4E-15
At5G46630	Clathrin adaptor complexes medium subunit family protein (AP2M)	2/2	2/2	4	1450	3.30E-141	151	1.7E-14
At4G23460	Adaptin family protein (AP1/2B2)	1/2	2/2	3	1170	3.30E-113	126	3.2E-12
At5G65960	Unknown	1/2	1/2	2	110	3.30E-07	87	4.6E-08

benthamiana. The combined transformation of AP1/2B1-nGFP and cGFP-AP2A1, AP1/2B1-cGFP and nGFP-AP2S, or AP1/2B1-cGFP and nGFP-AP2M resulted in fluorescent signals at the PM (Figure 2A), indicating that the two proteins interacted, whereas no interaction was found between AP2A1 and AP2S or between AP2A1 and AP2M in any of the combinations tested (see Supplemental Table 2 and Supplemental Figure 2 online).

In mammals, AP-2 functions in conjunction with clathrin (Boucrot et al., 2010). As none of the clathrin isoforms were retrieved in the TAP experiments, we tested whether AP-2 interacted with clathrin in vivo by performing coimmunoprecipitation experiments in *Arabidopsis* seedlings expressing *CLC2-GFP* (Konopka et al., 2008). Protein gel blot analysis with an antibody directed against the two AP2A proteins (Song et al., 2012) revealed that AP2A coimmunoprecipitated with CLC2-GFP (Figure 2B). Additional BiFC experiments validated that AP2A1 and clathrin (CLC2 and CHC) interacted with a GFP signal localized at the PM, in agreement with the coimmunoprecipitation data (Figure 2C; see Supplemental Table 2 and Supplemental Figure 2 online). In summary, the biochemical experiments confirm the predicted composition of the AP-2 core complex (Figure 2D; Bassham et al., 2008) in *Arabidopsis* and directly link this complex with clathrin, reinforcing the hypothesis that AP-2 is part of the CME machinery in plants.

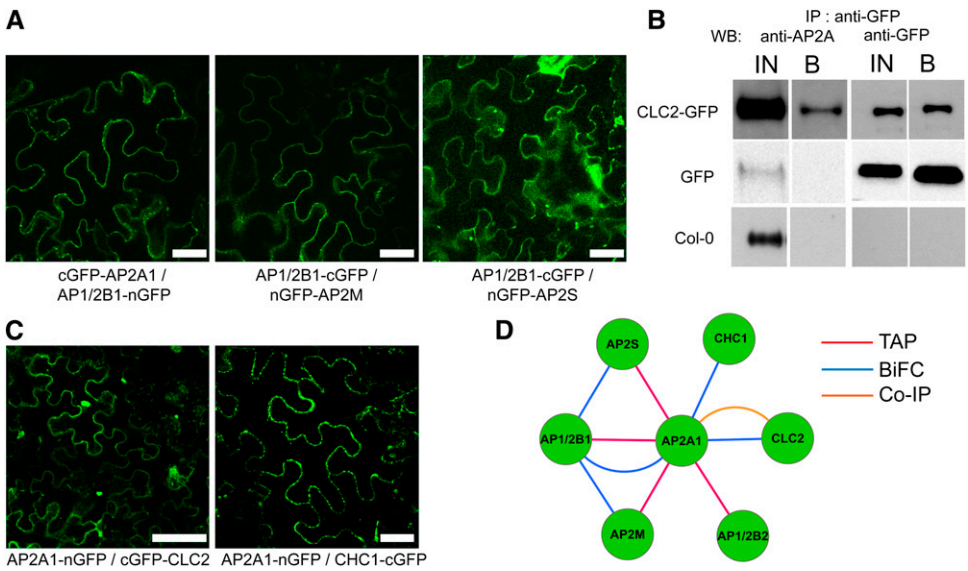

Figure 2. Identification of the *Arabidopsis* AP-2 Complex.

(A) and **(C)** BiFC assays in *N. benthamiana* depicting interactions (GFP signal) between AP1/2B1-nGFP and cGFP-AP2A1, AP1/2B1-cGFP and nGFP-AP2S, and AP1/2B1-cGFP and nGFP-AP2M **(A)** and between AP2A1-nGFP and cGFP-CLC2 and AP2A1-nGFP and CHC-cGFP (**C**). Bars = 20 μm.
(B) Coimmunoprecipitation of AP2A with CLC2-GFP. Total protein extracts of 7-d-old seedlings expressing *CLC2-GFP*, *GFP*, and the wild type (Col-0) were incubated with agarose-conjugated anti-GFP antibodies and probed with anti-GFP or anti-AP2A antibodies. IN is equivalent to 20% of the protein incubated with the beads for immunoprecipitation. IP, immunoprecipitation; WB, protein gel blot; IN, input; B, bound fraction.
(D) Schematic representation of the *Arabidopsis* AP-2 complex. Red, blue, and yellow lines represent interactions found via TAP, BiFC, and Co-IP, respectively. Co-IP, coimmunoprecipitation.

AP-2 Functions in CME at the PM

In mammals, AP-2 mediates endocytosis from the PM (Boucrot et al., 2010). To assess where AP-2 functions in the cell, we studied the AP-2 localization in *Arabidopsis* plants stably transformed with the large subunit AP2A1 fused to GFP under the control of the CaMV 35S promoter. Confocal microscopy imaging of epidermal cells of the *Arabidopsis* root meristem revealed that, besides a faint cytoplasmic distribution, both the C- and N-terminal AP2A1-GFP fusions mostly localized at the PM in a discontinuous fashion (Figure 3A; see Supplemental Figure 3 online). To exclude the possibility that the cellular localization of AP2A1-GFP was influenced by the fusion protein levels, we selected two independent transgenic lines (2-1 and 4-1) and analyzed the transcription of the transgene by quantitative real-time PCR (qRT-PCR). In both lines, the *AP2A1-GFP* expression was slightly higher or comparable to that of the endogenous *AP2A1* gene, namely, 0.75- and 0.42-fold for lines 2-1 and 4-1, respectively (see Supplemental Figure 3 online). The intact AP2A1-GFP fusion protein was also detected in both lines via protein gel blot analysis after immunoprecipitation with anti-GFP antibodies (see Supplemental Figure 3 online). Only the AP2A1-GFP line 2-1 was used hereafter. AP2A1-GFP colocalized with the lypophilic dye *N*-(3-triethylammoniumpropyl)-4-(6-(4-(diethylamino) phenyl) hexatrienyl) pyridinium dibromide (FM4-64) and CLC2-mCherry (Figures 3A and 3B) at the PM, but AP2A1 was found neither in CLC2-positive endosomes nor in FM4-64–stained endosomal compartments (Figures 3A and 3B).

Next, we investigated the possible role of AP-2 in endocytosis by interfering with several of its subunits through both

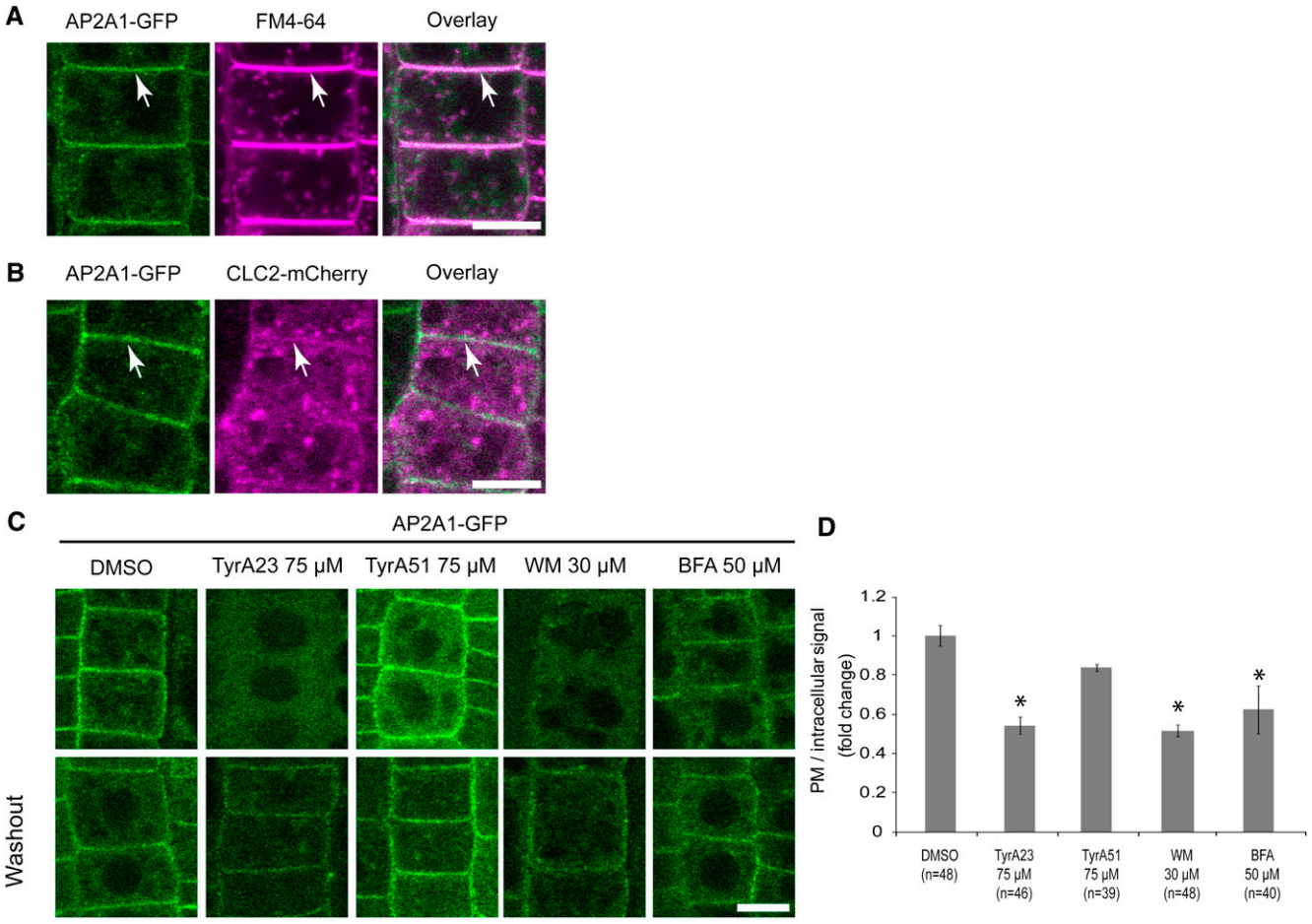

Figure 3. Localization of AP2A1 in *Arabidopsis* Roots.

(A) Discontinuous labeling of AP2A1-GFP (green) at the PM and colocalization with FM4-64 (magenta) at the PM (arrows).

(B) Colocalization of AP2A1-GFP with CLC2-mCherry at the PM in epidermal cells of the *Arabidopsis* root meristem. Arrows indicate colocalization at the PM.

(C) Dislodgement of AP2A1-GFP from the PM after treatment with Tyrphostin A23, Wortmannin, or BFA, but not Tyrphostin A51. 5-d-old seedlings were treated for 1 h with the drugs at the indicated concentrations. Bottom panels show recovery of the PM signal after a washout of 1 h with medium without drugs. TyrA23, Tyrphostin A23; TyrA51, Tyrphostin A51; WM, Wortmannin. Bars = 5 µm.

(D) Quantification of the ratio between the PM and the intracellular AP2A1-GFP signal intensities after treatments in **(C)**. Values were normalized against the DMSO control. Error bars indicate SD. P values (*t* -test), * < 0.05 relative to DMSO-treated control.

pharmacological and genetic approaches. Pharmacological inhibitors of endocytosis (Irani and Russinova, 2009; Irani et al., 2012), such as Wortmannin, Tyrphostin A23, and, to a minor extent, Brefeldin A (BFA), dislodged AP2A1-GFP from the PM in epidermal cells of *Arabidopsis* roots (Figure 3C; see Supplemental Figure 3 online), implying that the AP2A1-GFP localization at this compartment is required for endocytosis. Washout experiments restored the recruitment of AP2A1-GFP, indicating that the treatments did not interfere with the cell viability (Figure 3C).

To assess whether AP-2 functions in endocytosis, we generated a genetic knockdown of AP2A by constitutively expressing an RNA interference (RNAi) construct (*AP2A-RNAi*) that targeted the two *Arabidopsis* tandem-duplicated genes encoding AP2A, AP2A1 (At5g22770), and AP2A2 (At5g22780) (Bassham et al., 2008) (see Supplemental Figure 4 online). Additionally, a dominant-negative version of the medium AP2M subunit, designated AP2MΔC, was generated by deleting the C-terminal region responsible for the cargo binding (Owen and Evans, 1998). The *AP2MΔC* construct was expressed in *Arabidopsis* under an inducible promoter. In 7-d-old *Arabidopsis* seedlings that constitutively or conditionally expressed the *AP2A-RNAi* or the *AP2MΔC*, respectively, the main root was shorter than that of the wild type (see Supplemental Figure 4 online). Both AP-2 knockdown lines had a decreased uptake of the endocytic tracer FM4-64 in root epidermal cells analyzed by the number of FM4-64–labeled endosomes (Figures 4A and 4B). The dominant-negative effect of *AP2MΔC* expression was not limited to FM4-64 because the clathrin-dependent accumulation of another PM cargo, the auxin transporter PIN-FORMED2 (PIN2), in BFA bodies was also reduced in the AP2MΔC lines (see Supplemental Figure 5 online). In summary, the endocytic defects observed after targeting of the functionality of different AP-2 subunits strongly suggests that this complex plays a general role in endocytic events in plants.

AP-2 Regulates Endocytosis and Signaling of BRI1

Given the role played by AP-2 in the CME of PM receptor cargos in mammals (Boucrot et al., 2010) and the similarities between the *Arabidopsis* AP-2 and its mammalian counterpart, we evaluated whether AP-2 mediated the endocytosis of BRI1. BRI1-GFP colocalized with AP2A1-mTagRFP (see Supplemental Figure 3 online) at the PM (Figure 5A) in agreement with the reported receptor CME (Irani et al., 2012). Interaction between AP2A and BRI1 was also detected by coimmunoprecipitation in *Arabidopsis* seedlings expressing *BRI1-GFP*, as revealed by protein gel blot analysis with an anti-AP2A antibody (Song et al., 2012) (Figure 5B). Similarly, BRI1 and AP2A were coimmunoprecipitated in the presence of either brassinolide (BL) (100 nM, 1 h) or after incubation of the *BRI1-GFP*–expressing plants with the BR synthesis inhibitor brassinazole (2 μM, 24 h) to deplete the endogenous ligand (see Supplemental Figure 6 online). Pretreatment with brassinazole (2 μM, 24 h) followed by application of BL (100 nM, 1 h) to

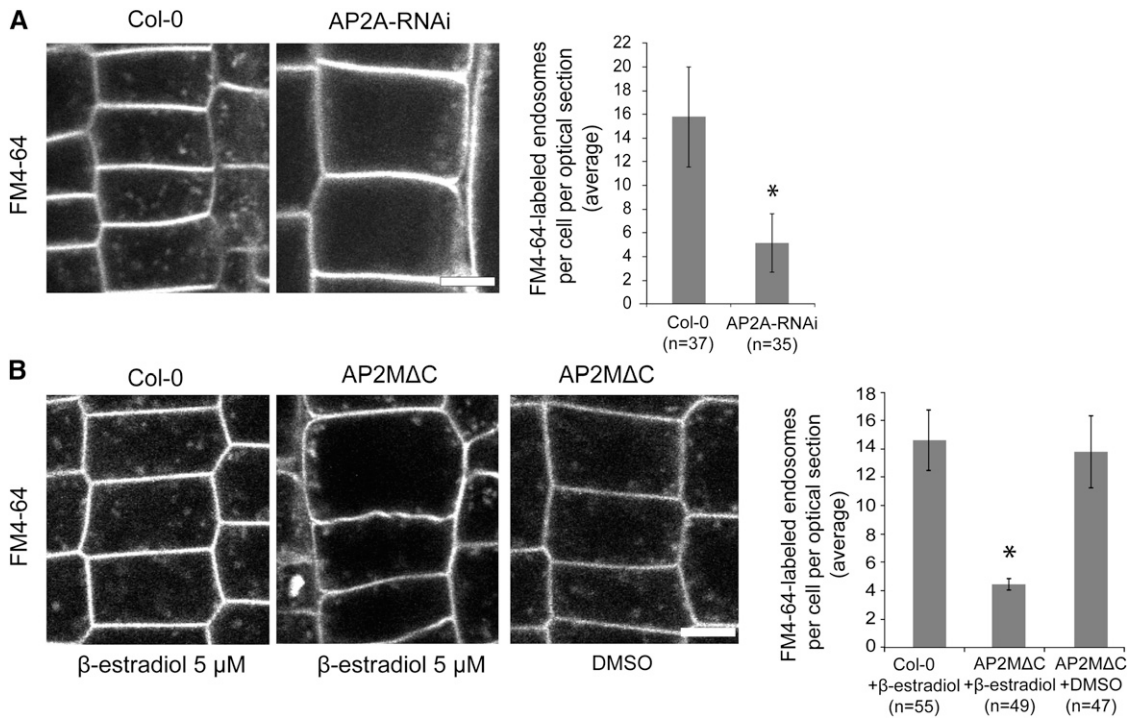

Figure 4. Functional Characterization of AP-2.

Impaired FM4-64 uptake in epidermal cells of the *Arabidopsis* root meristem constitutively expressing *AP2A-RNAi* **(A)** or after induction of *AP2MΔC* expression with 5 μM β-estradiol for 2 d **(B)**. Five-day-old seedlings were stained with FM4-64 (2 μM, 10 min) before imaging. Graphs represent total number of endosomes labeled by FM4-64 divided by the number of cells. Error bars indicate SD. P values (*t* test): * < 0.05 relative to Col-0 **(A)** and AP2MΔC after treatment with β-estradiol **(B)**. Bars = 5 μm.

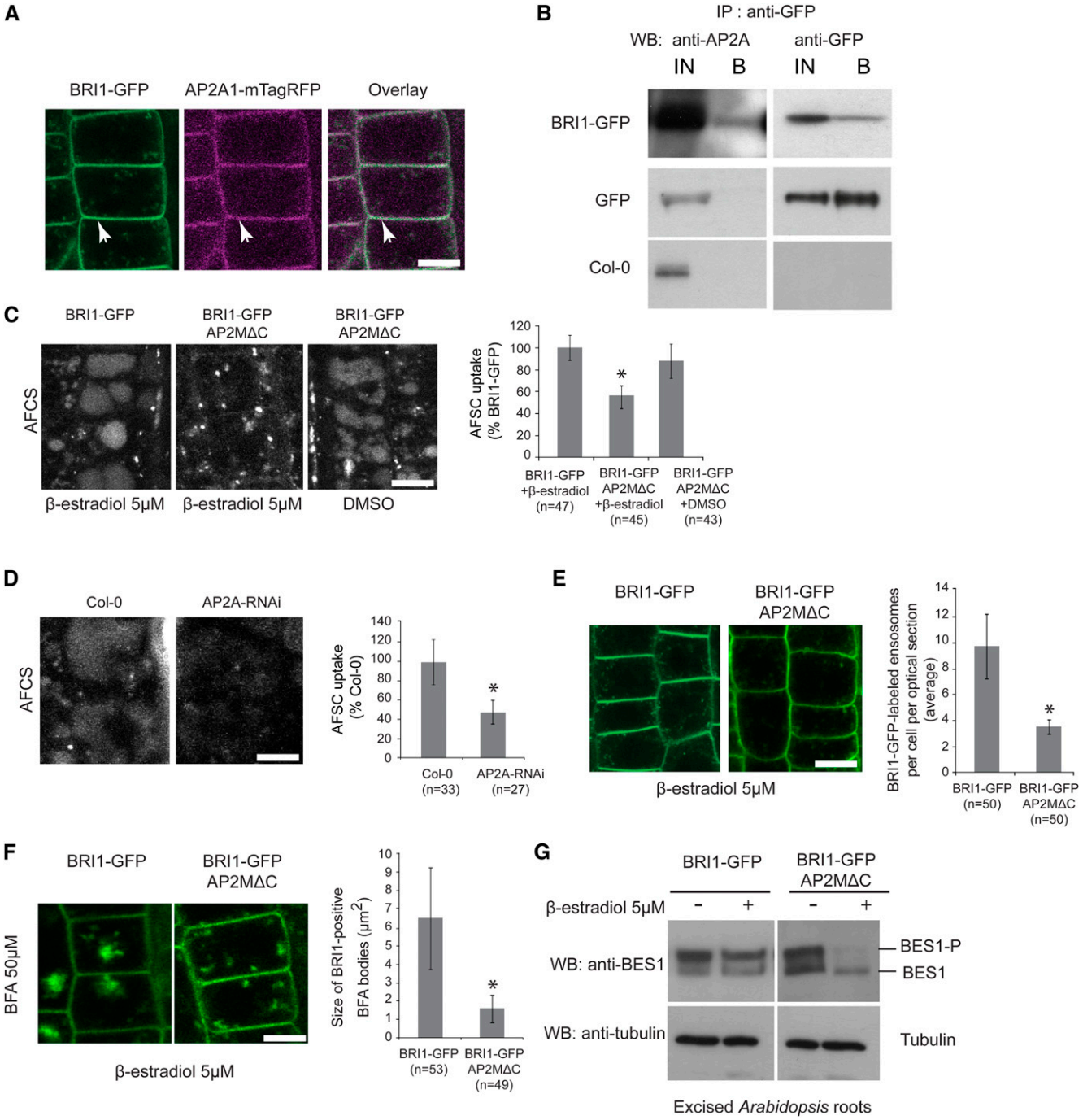

Figure 5. AP-2–Mediated BRI1 Endocytosis.

(A) Colocalization of BRI1-GFP with AP2A1-mTagRFP at the PM (arrow) in epidermal cells of the *Arabidopsis* root meristem.

(B) Coimmunoprecipitation of AP2A with BRI1-GFP. Total extracts of 7-d-old seedlings expressing *BRI1-GFP*, *GFP*, or the wild type (Col-0) were incubated with agarose-conjugated anti-GFP antibodies and probed with anti-AP2A or anti-GFP antibodies. IN is equivalent to 20% of the protein incubated with the beads for immunoprecipitation. IP, immunoprecipitation; WB, protein gel blot; IN, input; B, bound fraction.

(C) and **(D)** Reduced vacuolar accumulation of AFCS in epidermal cells of the root meristem by induced *AP2MΔC* expression (5 μM β-estradiol, 2 d) or constitutive AP2A silencing, respectively. Five-day-old *Arabidopsis* seedlings were pulsed for 30 min in 20 μM AFCS and imaged after a chase of 20 min. Graphs represent quantification of the vacuolar AFCS normalized to the *BRI1-GFP*–expressing line **(C)** or Col-0 **(D)**.

(E) Reduced number of BRI1-GFP–positive endosomes after induction of *AP2MΔC* expression (5 μM β-estradiol for 2 d). Graphs represent the average number of FM4-64–positive endosomes per cell.

activate the PM pool of BRI1 only led to similar results (see Supplemental Figure 6 online). Likewise, the interaction between BRI1 and CHC was not influenced by the availability of BRs (see Supplemental Figure 6 online). Thus, the recruitment of BRI1 into AP-2/clathrin-mediated endocytic processes is independent of its activation status.

The interaction between BRI1 and AP2A strongly implied an AP-2–dependent internalization of BRI1. As the BRI1 endocytosis can be followed by the internalization of fluorescently labeled BR Alexa Fluor castasterone (AFCS) (Irani et al., 2012), we analyzed the uptake of AFCS in root epidermal cells of *Arabidopsis* seedlings that expressed either the *AP2MΔC* or the *AP2A-RNAi* constructs, by quantifying the vacuolar accumulation of the dye after a chase of 20 min (Irani et al., 2012; Figure 5C; see Supplemental Figure 7 online). AFCS endocytosis was 45% lower in *AP2MΔC*-expressing cells than that in the control (Figure 5C). Similarly, the constitutive expression of *AP2A-RNAi* decreased the uptake of AFCS to 50% of the wild-type levels (Figure 5D), suggesting that a functional AP-2 is required for the BRI1 CME. These results were corroborated by introducing the dominant-negative *AP2MΔC* construct into *BRI1-GFP*–expressing *Arabidopsis* plants and monitoring the BRI1 endocytosis in the presence of the recycling inhibitor BFA. Inducible expression of *AP2MΔC* partially decreased the endosomal pool of BRI1-GFP in epidermal cells of *Arabidopsis* roots (Figure 5E) and significantly reduced the size of the BRI1-GFP–labeled BFA bodies, denoting an impaired protein trafficking from the PM (Figure 5F).

In plants, endocytosis of PM receptors has been linked to the regulation of their signaling activity (Di Rubbo and Russinova, 2012). Previously, inhibition of BRI1 endocytosis at the PM had been shown to enhance BR signaling, monitored by the phosphorylation status of the key BR transcription factor BRI1-EMS-SUPPRESSOR1 (BES1)/BRASSINAZOLE RESISTANT2 (BZR2) (Irani et al., 2012). Protein gel blot analysis of total protein extracts of excised *Arabidopsis* roots after induction of *AP2MΔC* expression revealed that BES1/BZR2 was dephosphorylated (Figure 5G), hinting at an enhanced BR signaling. This result was validated by a qRT-PCR analysis of the expression of the BR-regulated genes *DWARF4* (*DWF4*) and *EXPANSINA8* (*EXPA8*), both identified as direct targets of the transcription factors BZR1 and/or BES1/BZR2 (Sun et al., 2010; Yu et al., 2011). As expected, upon BR signaling activation, *DWF4* and *EXPA8* were downregulated and upregulated, respectively, after induction of *AP2MΔC* (see Supplemental Figure 8 online). Taken together, our data show that AP-2 associates with BRI1 and regulates its endocytosis, consequently regulating the signaling output of the receptor.

DISCUSSION

AP-2 Is Part of the Clathrin Assembly Machinery at the PM in *Arabidopsis*

Similar to the mammalian system, CME appears to be a major internalization route in plants hinting at a good conservation of the endocytic machinery (Chen at al., 2011). Indeed, our TAP experiments confirmed that the composition of the *Arabidopsis* AP-2 complex is similar to its mammalian counterpart (Bassham et al., 2008). Four types of proteins (AP2A, AP1/2B, AP2M, and AP2S), representing the core complex, were identified in every purification, suggesting a stable interaction. The fact that two different AP1/2B subunits (At4g11380 and At4g23460) were found in the TAP eluates implies that, as shown for the mammalian system (Page and Robinson, 1995), the AP1/2B subunits in *Arabidopsis* might be shared with AP-1, as confirmed by the composition of AP-1 and AP-3 in *Arabidopsis*, in which the same AP1/2B subunits had been identified as part of AP-1, but not of AP-3 (Zwiewka et al., 2011; Teh et al., 2013).

In accordance with its putative function in CME, AP-2 coimmunoprecipitated with CLC2, although clathrin was not detected in any of the TAP experiments. The TAP results revealed that this technology could differ in its ability to identify core components. The transient nature of the clathrin–AP-2 association at the PM (Cocucci et al., 2012) might explain the absence of clathrin in our TAP experiments.

In contrast with the previously reported localization of the *Arabidopsis* AP2M subunit in Golgi and TGN compartments (Happel et al., 2004), the GFP-tagged AP2A1 localized at the PM and the cytoplasm. Although we cannot exclude that some of the faint cytoplasmic signals of AP2A1 correspond to TGN/early endosome compartments, the observed BiFC interactions between different AP-2 subunits or between clathrin and AP2A1 at the PM support the PM localization of AP2A1. In addition, pharmacological dislodgement of AP2A1-GFP from the PM by means of endocytic inhibitors also suggests a role for AP-2 in endocytosis at this compartment. This hypothesis was strengthened by the impaired endocytosis at the PM of FM4-64, AFCS, BRI1-GFP, and PIN2 due to the genetic interference with the AP-2 complex function through the expression of either *AP2A-RNAi* or dominant-negative *AP2MΔC* constructs. As BRI1 and PIN2 undergo CME (Dhonukshe et al., 2007; Irani et al., 2012), impairment of their internalization points toward an AP-2 involvement in CME, again in agreement with its expected function. The AP2A1-GFP localization displays striking similarities with that of T-PLATE, another putative clathrin adaptor protein. Both proteins interact with clathrin and react similarly to endocytic drugs (Van Damme et al., 2011). However, it remains to be determined whether the

Figure 5. (continued).

(F) Reduced size of the BRI1-labeled BFA bodies after induction of *AP2MΔC* expression (5 μM β-estradiol for 2 d). Five-day-old seedlings were treated with BFA (50 μM, 1 h). Graphs represent the sizes of the BRI1-GFP–positive BFA bodies. Error bars indicate SD. P values (*t* test): * < 0.05 relative to the *BRI1-GFP*–expressing line after treatment with β-estradiol (**[C]**, **[E]**, and **[F])** and Col-0 **(D)**. Bars = 5 μm.

(G) Protein gel blot analysis of 7-d-old *Arabidopsis* seedlings expressing *BRI1-GFP* in Col-0 or in an AP2MΔC background after DMSO or β-estradiol treatment (5 μM for 2 d), probed with anti-BES1 or antitubulin antibodies.

two proteins work together in CME or are part of two different clathrin assembly machineries at the PM.

AP-2 Mediates Endocytosis of BRI1 and Regulates BR Signaling

The AP-2 complex regulates BR receptor endocytosis because the expression of the *AP2A-RNAi* and *AP2MΔC* constructs block the internalization of BRI1-GFP and its fluorescent ligand AFCS. Although BRI1 coimmunoprecipitated with AP2A in vivo, the BRI1-GFP purification protocol did not distinguish between different cellular membranes. Yet, the localization of AP2A1-GFP at the PM hints at a plausible BRI1–AP-2 interaction at the PM. AP-2 interacted with BRI1 independently of the presence or absence of BRs, reconfirming that BRI1 activation is not required for its endocytosis (Geldner et al., 2007). Nevertheless, the activation status of BRI1 has been coupled indirectly to endocytosis because association with the coreceptor BRI1 ASSOCIATED RECEPTOR KINASE1 as well as dephosphorylation of the receptor itself have been linked to BRI1 trafficking (Russinova et al., 2004; Wu et al., 2011). Hence, some phosphorylated residues in BRI1 or particular phosphorylation patterns might play a role in endocytosis, independently or additionally to their contribution in BR signaling activation. Therefore, phosphorylation, together with other posttranslational modifications as well, might be good candidates to investigate the mechanism by which BRI1 is recruited into the clathrin cages.

In mammalian systems, the interaction between AP-2 and the cargo proteins relies on the presence of either the YxxΦ or dileucine endocytic motifs in the cargos (Bonifacino and Traub, 2003; Traub, 2009). Although both TyrxxΦ and dileucine motifs have been mapped to plant PM proteins, of which some undergo endocytosis (Geldner and Robatzek, 2008), only TyrxxΦ motifs have been linked to a role in endocytosis. Tyr-to-Ala substitutions in TyrxxΦ interfered with endocytosis of the tomato receptor EIX2 and BOR1 (Bar and Avni, 2009; Takano et al., 2010). In addition, AP2M binds to VSR-PS1 via a TyrxxΦ motif in vitro (Happel et al., 2004). In BRI1, putative TyrxxΦ motifs are located in the intracellular kinase domain (Geldner and Robatzek, 2008), in contrast with the mammalian cargo receptors in which functional endocytic motifs are present either at the C-terminal tail (Jiang et al., 2003) or in the region proximal to the transmembrane domain (Ehrlich et al., 2001). As the contributions of neither the kinase activity nor the phosphorylation sites for the BRI1 endocytosis are known, it would be essential to test whether these motifs participate in the interaction with AP-2. Sequence analysis did not predict canonical dileucine motifs on the intracellular domain of BRI1 (Geldner and Robatzek, 2008). Therefore, the motifs responsible for the interaction between BRI1 and AP-2 remain unknown. One possibility is that AP-2 recognizes noncanonical motifs in the cargo proteins, of which the sequences have not yet been identified. A second possible scenario is that an unknown internalization motif-carrying factor (a BRI1 coreceptor or another BRI1-interacting protein) is recognized by AP-2 and, in turn, bridges the interaction with BRI1. This second hypothesis would benefit from a proteomics approach to detect new interactors of BRI1 that are not directly involved in BR signaling.

Partial blocking of the AP-2 function impaired BRI1 endocytosis and, simultaneously, enhanced BR signaling, as shown by the increased dephosphorylation of the BR transcription factor BES1/BZR2 (Yin et al., 2002) and the effect on the transcription of the BR-regulated genes *DWF4* and *EXPA8* (Sun et al., 2010; Yu et al., 2011). Because the expression of *AP2A-RNAi* and *AP2MΔC* constructs did not result in abnormal accumulation of BRI1-GFP in endosomal compartments, we conclude that the enhanced BR signaling depends on the PM pool of BRI1 and that the AP-2–mediated endocytosis of BRI1 negatively regulates the BRI1 signaling. These data are in agreement with previous reports in which CME is a negative regulator of BR signaling (Irani et al., 2012). However, except for the reduced main root, the growth phenotypes of 7-d-old plants expressing *AP2MΔC* and *AP2A-RNAi* could not be linked directly to the phenotypes caused by an enhanced BR signaling and reported in *Arabidopsis* plants overexpressing the BR receptor *BRI1* (Friedrichsen et al., 2000; Wang et al., 2001) and overproducing BRs by overexpression of the *DWF4* gene (Wang et al., 2001), or in *bes1-D* plants carrying a gain-of-function mutation in the BES1 transcription factor (Yin et al., 2002). Interestingly, previous studies (González-García et al., 2011) have shown that *BRI1*-overexpressing and *bes1-D* plants display reduced roots because a balanced BR signaling is required to regulate growth. Conversely, AP-2 appears to be involved in the endocytosis of other PM cargos, suggesting that other signaling pathways will also be impaired in the AP-2 knockdown mutants. Therefore, the growth defects observed in plants expressing *AP2MΔC* and *AP2A-RNAi* might not be a consequence of BR signaling activation only. Strongly inhibited growth and development were observed in seedlings expressing endocytic inhibitors (i.e., the dominant-negative clathrin HUB or GDP-locked and inactive Rab5 GTPase homolog ARA7) (Dhonukshe et al., 2008; Kitakura et al., 2011). In these mutant backgrounds, BRI1 endocytosis was blocked completely and BR signaling was strongly enhanced (Irani et al., 2012). Identifying tools for selective inhibition of BRI1 endocytosis, possibly by exploring chemical genomics, will allow us to assess the BR-related phenotypes caused by the interference with BRI1 endocytosis.

METHODS

Plant Material and Growth Conditions

Arabidopsis thaliana (accession Columbia-0 [Col-0]) seedlings were stratified for 2 d at 4°C and germinated on vertical agar plates with half-strength Murashige and Skoog (1/2MS) medium with 1% (w/v) Suc at 22°C in a 16-h/8-h light/dark cycle for 4 d. Liquid 1/2MS medium was used for all assays and treatments. BRI1-GFP (Friedrichsen et al., 2000) and CLC2-GFP (Konopka et al., 2008) were described previously. BRI1-GFP/AP2MΔC and BRI1-GFP/AP2A1-mTagRFP plants were generated by floral dip (Clough and Bent, 1998) in a BRI1-GFP background (Friedrichsen et al., 2000). BRI1-GFP/CLC2-mCherry and AP2A1-GFP/CLC2-mCherry lines were generated by crossing CLC2-mCherry into BRI1-GFP and into AP2A1-GFP, respectively, and selected by antibiotic resistance and fluorescent signals.

For induction of estradiol-inducible constructs, seedlings were germinated on 1/2MS plates and transferred to 1/2MS plates containing 5 μM estradiol (Sigma-Aldrich) 4 d after germination. Expression of dominant-negative AP2M was checked by qRT-PCR with primers listed in

Supplemental Table 3 online. For *AP2A-RNAi*–expressing lines, the effective blocking of *AP2A1* and *AP2A2* expression was monitored by qRT-PCR using primers directed against both transcripts. The expression levels were normalized to the expression of the elongation factor *EEF1α4* (At5g60390) (see Supplemental Table 3 online).

Construct Preparation

The AP2A1 (At5g22770), AP1/2B1 (At4g11380), AP2M (At4g46630), and AP2S (At1g47830) subunits were amplified from cDNA clones obtained from the ABRC by PCR with KaPaHIFI polymerase (Sopachem) and added to the Gateway system–compatible attB sites (Invitrogen). To generate transgenic plants with both *AP2A1* (At5g22770) and *AP2A2* (At5g22780) genes suppressed simultaneously, an RNAi construct was designed using a DNA fragment with the nucleotide positions 150 to 699 of *AP2A1* that shows an identical sequence to the corresponding regions of the two *AP2A* genes. The DNA fragment was isolated by PCR with primers aRNAi-5′ and aRNAi-3′ and inserted into the pENTER vector with the *Xho*I and *Acc*65I restriction sites and subsequently transferred to pHellgate8 via LR clonase (Invitrogen) to generate the pHellsgate-a-RNAi construction.

The AP2MΔC was cloned into pMDC7 (Brand et al., 2006). AP2A1 was cloned into pKCTAP and pKNTAP as described previously (Van Leene et al., 2007) and in pKFGW2 or pKGWF2 (Karimi et al., 2007) to generate the *35Spro*:*AP2A1-GFP* and *35Spro*:*GFP-AP2A1* constructs, respectively. The *RPS5Apro*:*AP2A1-mTagRFP* construct was generated by recombining pENL1-L2AP2A1, pENL4-L1r-pRPS5A, pENRp2rp2-mTagRFP, and pB7m34GW (Karimi et al., 2007). Gateway technology (Invitrogen) was used for cloning.

The BiFC constructs of AP2A1, AP1/2B1, AP2M, AP2S, CHC, and CLC2 were generated as described by Boruc et al. (2010) and Van Damme et al. (2011). cGFP or nGFP (Boruc et al., 2010) were amplified from pKFGW2 by PCR with KaPaHIFI polymerase (Sopachem) added to the Gateway system–compatible attB sites (Invitrogen) and recombined into pDONR221. Expression clones were generated in the pH2GW7 and pK2GW7 destination vectors (Karimi et al., 2007).

TAP

Cloning of transgenes encoding tag fusions under the control of the constitutive CaMV 35S promoter and transformation of *Arabidopsis* cell suspension cultures were performed as previously described (Van Leene et al., 2007). TAP experiments of protein complexes were done with the GS tag (Bürckstümmer et al., 2006), followed by protein precipitation and separation, according to Van Leene et al. (2008). For the protocols of proteolysis and peptide isolation, acquisition of mass spectra by a 4800 Proteomics Analyzer (Applied Biosystems), and mass spectrometry–based protein homology identification from the genomic database of The Arabidopsis Information Resource, we refer to Van Leene et al. (2010). Experimental background proteins were subtracted based on ~40 TAP experiments on wild-type cultures and cultures expressing the TAP-tagged mock proteins β-glucuronidase, red fluorescent protein (RFP), and GFP (Van Leene et al., 2010) (see Supplemental Methods 1 online).

BiFC

Agrobacterium tumefaciens–mediated transient transformation of *Nicotiana benthamiana* leaves and imaging for BiFC experiments were done as described (Boruc et al., 2010) with minor modifications. In brief, *Agrobacterium* strains transformed with the BiFC constructs were grown for 2 d in yeast extract broth medium, resuspended in infiltration buffer (0.5 mM MES, 1 mM $MgCl_2$, and 100 μM acetosyringone) at the final optical density at 600 nm (OD_{600}) value of 1. Prior to the leaf infiltration, 300 mL of each bacterial culture was mixed for a total volume of 900 mL and infiltrated into leaves of 4-week-old *N. benthamiana* plants. Leaves were imaged and processed for qRT-PCR 4 d after infiltration. The background levels of autofluorescence used to set the GFP signal threshold level were acquired in *N. benthamiana* leaves coexpressing the nontagged cGFP and nGFP constructs. Look-up table and laser power were set to exclude fluorescent signals equal or lower than the threshold. Combinations were scored as positive interactions when the GFP signal was above the threshold.

Immunoprecipitation and Protein Gel Blot Analysis

Ten-day-old plants expressing *BRI1-GFP* or *CLC2-GFP* were treated for 1 h with 100 nM BL in liquid 1/2MS medium. Seedlings were homogenized in liquid nitrogen and extracted in a subcellular extraction buffer (SEB; 250 mM Suc, 20 mM HEPES, pH 7.4, 10 mM KCl, 1.5 mM $MgCl_2$, 1 mM EDTA, 1 mM EGTA, 1% Nonidet P-40, 0.1% Na-deoxycholate, 100 mM DTT, 1 mM phenylmethylsulfonyl fluoride, EDTA-free protease inhibitor cocktail complete [Roche], and phosphatase inhibitors [Phospho-STOP; Roche]; adapted from http://www.abcam.com/index.html?pageconfig=resource&rid=11385). Proteins were quantified by the Bradford method (Bio-Rad) of which 3 mg at a concentration of 5 mg/mL was incubated with 5 μL of washed, SEB-equilibrated GFP-Trap beads (ChromoTek) for 4 h at 4°C. Beads were washed four times in SEB, resuspended, and boiled in loading buffer. Half the beads and 15 μL of the input fraction, equivalent to 20% of the protein incubated with the beads, were separated on 7% NuPAGE gels (Invitrogen), blotted onto polyvinylidene difluoride membranes, blocked (with 3% skimmed milk powder in Tris-buffered saline), and detected with rabbit polyclonal anti-AP2A antibodies (1:1000) (Song et al., 2012), horseradish peroxidase (HRP)–conjugated anti-rabbit secondary antibodies (1:10,000; GE-Healthcare), and HRP-conjugated mouse anti-GFP antibodies (1:40,000; Miltenyi Biotec) via enhanced chemiluminescence (ECL plus; GE-Healthcare). Blots were stripped with 50 mM Gly-HCl, pH 2.5, and 5% SDS for 2 min and reprobed for clathrin with anti-CHC antibodies (1:500; Santa Cruz Biotechnologies) and anti-mouse polyclonal antibodies (NA931V; GE Healthcare). Full scans of the immunoblots are presented (see Supplemental Figure 9 online).

Chemical Treatments

Treatments were 100 nM BL (Fuji Chemical Industries), 30 μM Wortmannin, 75 μM Tyrphostin A23, 75 μM Tyrphostin A51, 50 μM BFA, or 2 μM Concanamycin A (Sigma-Aldrich) on 5-d-old seedlings in liquid 1/2MS medium for 1 h before imaging or protein extraction. For expression of estradiol-inducible constructs, 3-d-old seedlings were transferred to agar plates with 1/2MS medium containing 10 μM β-estradiol (Sigma-Aldrich) and analyzed after 2 d.

BES Dephosphorylation Assay

For BES1 dephosphorylation studies, roots from 7-d-old *Arabidopsis* seedlings were homogenized in liquid nitrogen. Total proteins were extracted (20 mM Tris-HCl, 150 mM NaCl, 1% SDS, 100 mM DTT, and EDTA-free protease inhibitor cocktail complete [Roche]) and quantified with the Quick start Bradford protein assay (1× Bradford dye reagent) (Bio-Rad). Proteins (35 μg) were separated on 10% SDS-PAGE gels and blotted onto polyvinylidene difluoride membranes using the iBlot system (Invitrogen). For blocking and antibody dilutions, 3% skimmed milk powder in Tris-buffered saline was used. BES1 was detected with rabbit polyclonal anti-BES1 antibodies10 (1:1000) and HRP-conjugated anti-rabbit antibodies (1:10,000; GE Healthcare). Signals were detected with ECL plus (GE-Healthcare). Full scans of the immunoblots are presented (see Supplemental Figure 7 online).

Confocal Imaging and AFCS Uptake Quantification

N. benthamiana leaves and *Arabidopsis* seedlings were imaged on a confocal laser scanning microscope (FluoView 1000; Olympus) with a 60× water immersion lens (numerical aperture of 1.2) at digital zoom 3. AFCS was taken up as described previously (Irani et al., 2012). In brief, five 4-d-old seedlings were dipped in a 200-μL droplet of ligand. Seedlings were pulsed for 30 min and washed three times for 10 s and chased for 10 or 20 additional min. Washing and chasing steps were done with 1/2MS medium. To measure the fluorescence signals in vacuoles, stacks of a minimum of four 2.5-μm slices were obtained covering more than 10 μm of the epidermal cells. Four slices covering the epidermal cell layer were merged with maximum projection. The signal intensity of the elliptical region of interest was quantified with ImageJ (http://rsbweb.nih.gov/ij/) and normalized to the area.

Immunodetection was done as described (Sauer et al., 2006) with the antibodies anti-PIN2 (1:1000) (Abas et al., 2006) and anti-rabbit-Cy3 (1:600; Sigma-Aldrich). Full-size confocal pictures are presented (see Supplemental Figure 10 online).

qRT-PCR Analysis

Total RNA was extracted from 20 5-d-old *Arabidopsis* seedlings or from *N. benthamiana* leaves transiently expressing different BiFC constructs with the RNeasy kit (Qiagen). Total RNA (1 μg) was used for preparation of cDNA (iScript cDNA synthesis kit) according to the manufacturer's protocol (Bio-Rad) and diluted 10 times. qRT-PCR analysis of *GFP*, *DWF4*, *EXPA8*, *AP2M*, *AP2A1*, and *AP2A2* genes was done with SYBR® Green I Master kit (Roche Diagnostics) on a LightCycler 480 (Roche Diagnostics) with the primers listed in Supplemental Table 3 online. Normalization was done against the average cycle threshold value of the housekeeping gene *EF1BB* (At1G30230). "Ct" refers to the number of cycles at which SYBR® Green fluorescence reaches an arbitrary value during the exponential phase of the cDNA amplification. Each run contained three technical repeats per sample, and experiments were repeated in two biological replicates, except for the tobacco infiltration experiment where three technical repeats were used. Graphs in figures represent one biological repeat.

Accession Numbers

Sequence data from this article can be found in the Arabidopsis Genome Initiative or GenBank/EMBL databases under the following accession numbers: At5g22770 (AP2A1), At5g22780 (AP2A2), At4g11380 (AP1/2B1), At4g23460 (AP1/2B2), At4g46630 (AP2M), At1g47830 (AP2S), At4g39400 (BRI1), At2g40060 (CLC2), At5g65960, At3G50660 (DWF4), and At2G40610 (EXPA8). The supplemental data are deposited in the DRYAD repository at http://dx.doi.org/10.5061/dryad.57r3c.

Supplemental Data

The following materials are available in the online version of this article.

Supplemental Figure 1. Acrylamide Gel Separation of Proteins Copurified with the AP2A1-TAP Bait.

Supplemental Figure 2. Negative Controls for Bimolecular Fluorescent Complementation Experiments.

Supplemental Figure 3. Localization of AP2A1 in *Arabidopsis*.

Supplemental Figure 4. Characterization of *Arabidopsis* Lines Expressing *AP2A-RNAi* and *AP2MΔC*.

Supplemental Figure 5. Impaired PIN2 Endocytosis by the Expression of the *AP2MΔC* Dominant-Negative Construct.

Supplemental Figure 6. BRI1-GFP Coimmunoprecipitation with AP2A and CHC Independent of the Ligand Availability.

Supplemental Figure 7. Reduced AFCS Uptake in *Arabidopsis* Lines Expressing *AP2A-RNAi* and *AP2MΔC*.

Supplemental Figure 8. Enhanced BR Signaling after the Inducible *AP2MΔC* Expression.

Supplemental Figure 9. Full Scans of Immunoblots.

Supplemental Figure 10. Full-Size Confocal Images.

Supplemental Table 1. Peptide Mass Fingerprinting and Mass Spectroscopy Data for TAP Experiments.

Supplemental Table 2. Protein–Protein Interactions Tested by BiFC.

Supplemental Table 3. Primers Used.

Supplemental Methods 1. Protein Identification.

ACKNOWLEDGMENTS

We thank Yanhai Yin for sharing BES1 antibodies, Sebastian Bednarek for the CLC2-GFP line and the CLC2 clone, Wim Grunewald for the pENL4-L1r-pRPS5 clone, Jarne Pawels for technical assistance, Steffen Vanneste for useful suggestions and technical assistance in AP2A1 localization, and Martine De Cock for help in preparing the article. This work was supported by the Marie-Curie Initial Training Network Bravissimo (PITN-GA-2008-215118; to E.R.), the Odysseus program of the Research Foundation-Flanders and European Research Council Starting Grant (ERC-2011-Stg-20101109; to J.F.), and the Advanced Biomass R&D Center funded by the Ministry of Education, Science, and Technology (2012055057) (Korea) (to I.W.). A.G. and W.D. are indebted to the Agency for Innovation by Science and Technology for predoctoral fellowships. D.V.D. is a postdoctoral fellow of the Research Foundation-Flanders.

AUTHOR CONTRIBUTIONS

S.D.R., N.G.I., and E.R. conceived the study and designed the experiments. S.D.R., N.G.I., S.Y.K., Z.-Y.X., A.G., W.D., I.H., I.V., G.P., D.E., S.S., K.S., J.K.-V., J.F., G.D.J., and D.V.D. generated lines and constructs and performed the experiments. N.G.I., S.Y.K., I.V., G.P., D.E., G.D.J., and E.R. analyzed the data. S.D.R. and E.R. wrote the article. All authors revised the article.

Received May 31, 2013; revised July 22, 2013; accepted August 6, 2013; published August 23, 2013.

REFERENCES

Abas, L., Benjamins, R., Malenica, N., Paciorek, T., Wiśniewska, J., Moulinier-Anzola, J.C., Sieberer, T., Friml, J., and Luschnig, C. (2006). Intracellular trafficking and proteolysis of the *Arabidopsis* auxin-efflux facilitator PIN2 are involved in root gravitropism. Nat. Cell Biol. **8:** 249–256. Erratum. Nat. Cell Biol. **8,** 424.

Adam, T., Bouhidel, K., Der, C., Robert, F., Najid, A., Simon-Plas, F., and Leborgne-Castel, N. (2012). Constitutive expression of clathrin hub hinders elicitor-induced clathrin-mediated endocytosis and defense gene expression in plant cells. FEBS Lett. **586:** 3293–3298.

Bar, M., and Avni, A. (2009). EHD2 inhibits ligand-induced endocytosis and signaling of the leucine-rich repeat receptor-like protein LeEix2. Plant J. **59:** 600–611.

Barberon, M., Zelazny, E., Robert, S., Conéjéro, G., Curie, C., Friml, J., and Vert, G. (2011). Monoubiquitin-dependent endocytosis of the IRON-REGULATED TRANSPORTER 1 (IRT1) transporter controls iron uptake in plants. Proc. Natl. Acad. Sci. USA **108:** 12985–12986 (E450–E458).

Barth, M., and Holstein, S.E.H. (2004). Identification and functional characterization of *Arabidopsis* AP180, a binding partner of plant αC-adaptin. J. Cell Sci. **117:** 2051–2062.

Bassham, D.C., Brandizzi, F., Otegui, M.S., and Sanderfoot, A.A. (2008). The secretory system of Arabidopsis. In The Arabidopsis Book **6:** e0116, doi/10.1199/tab.0116.

Bonifacino, J.S., and Traub, L.M. (2003). Signals for sorting of transmembrane proteins to endosomes and lysosomes. Annu. Rev. Biochem. **72:** 395–447.

Boruc, J., Van den Daele, H., Hollunder, J., Rombauts, S., Mylle, E., Hilson, P., Inzé, D., De Veylder, L., and Russinova, E. (2010). Functional modules in the *Arabidopsis* core cell cycle binary protein-protein interaction network. Plant Cell **22:** 1264–1280.

Boucrot, E., Saffarian, S., Zhang, R., and Kirchhausen, T. (2010). Roles of AP-2 in clathrin-mediated endocytosis. PLoS ONE **5:** e10597.

Brand, L., Hörler, M., Nüesch, E., Vassalli, S., Barrell, P., Yang, W., Jefferson, R.A., Grossniklaus, U., and Curtis, M.D. (2006). A versatile and reliable two-component system for tissue-specific gene induction in Arabidopsis. Plant Physiol. **141:** 1194–1204.

Bürckstümmer, T., Bennett, K.L., Preradovic, A., Schütze, G., Hantschel, O., Superti-Furga, G., and Bauch, A. (2006). An efficient tandem affinity purification procedure for interaction proteomics in mammalian cells. Nat. Methods **3:** 1013–1019.

Chen, X., Irani, N.G., and Friml, J. (2011). Clathrin-mediated endocytosis: The gateway into plant cells. Curr. Opin. Plant Biol. **14:** 674–682.

Clough, S.J., and Bent, A.F. (1998). Floral dip: A simplified method for *Agrobacterium*-mediated transformation of *Arabidopsis thaliana*. Plant J. **16:** 735–743.

Cocucci, E., Aguet, F., Boulant, S., and Kirchhausen, T. (2012). The first five seconds in the life of a clathrin-coated pit. Cell **150:** 495–507.

Collins, B.M., McCoy, A.J., Kent, H.M., Evans, P.R., and Owen, D.J. (2002). Molecular architecture and functional model of the endocytic AP2 complex. Cell **109:** 523–535.

Dhonukshe, P., Aniento, F., Hwang, I., Robinson, D.G., Mravec, J., Stierhof, Y.-D., and Friml, J. (2007). Clathrin-mediated constitutive endocytosis of PIN auxin efflux carriers in *Arabidopsis*. Curr. Biol. **17:** 520–527.

Dhonukshe, P., et al. (2008). Generation of cell polarity in plants links endocytosis, auxin distribution and cell fate decisions. Nature **456:** 962–966.

Di Rubbo, S., and Russinova, E. (2012). Receptor-mediated endocytosis in plants. In Plant Endocytosis, J. Šamaj, ed. (Heidelberg, Germany: Springer), pp. 151–164.

Ehrlich, M., Shmuely, A., and Henis, Y.I. (2001). A single internalization signal from the di-leucine family is critical for constitutive endocytosis of the type II TGF-β receptor. J. Cell Sci. **114:** 1777–1786.

Friedrichsen, D.M., Joazeiro, C.A.P., Li, J., Hunter, T., and Chory, J. (2000). Brassinosteroid-insensitive-1 is a ubiquitously expressed leucine-rich repeat receptor serine/threonine kinase. Plant Physiol. **123:** 1247–1256.

Geldner, N., Hyman, D.L., Wang, X., Schumacher, K., and Chory, J. (2007). Endosomal signaling of plant steroid receptor kinase BRI1. Genes Dev. **21:** 1598–1602.

Geldner, N., and Robatzek, S. (2008). Plant receptors go endosomal: A moving view on signal transduction. Plant Physiol. **147:** 1565–1574.

González-García, M.-P., Vilarrasa-Blasi, J., Zhiponova, M., Divol, F., Mora-García, S., Russinova, E., and Caño-Delgado, A.I. (2011). Brassinosteroids control meristem size by promoting cell cycle progression in *Arabidopsis* roots. Development **138:** 849–859.

Happel, N., Höning, S., Neuhaus, J.-M., Paris, N., Robinson, D.G., and Holstein, S.E.H. (2004). *Arabidopsis* μA-adaptin interacts with the tyrosine motif of the vacuolar sorting receptor VSR-PS1. Plant J. **37:** 678–693.

Hirst, J., Barlow, L.D., Francisco, G.C., Sahlender, D.A., Seaman, M.N.J., Dacks, J.B., and Robinson, M.S. (2011). The fifth adaptor protein complex. PLoS Biol. **9:** e1001170.

Holstein, S.E.H., Drucker, M., and Robinson, D.G. (1994). Identification of a β-type adaptin in plant clathrin-coated vesicles. J. Cell Sci. **107:** 945–953.

Irani, N.G., and Russinova, E. (2009). Receptor endocytosis and signaling in plants. Curr. Opin. Plant Biol. **12:** 653–659.

Irani, N.G., et al. (2012). Fluorescent castasterone reveals BRI1 signaling from the plasma membrane. Nat. Chem. Biol. **8:** 583–589.

Ito, E., Fujimoto, M., Ebine, K., Uemura, T., Ueda, T., and Nakano, A. (2012). Dynamic behavior of clathrin in *Arabidopsis thaliana* unveiled by live imaging. Plant J. **69:** 204–216.

Jackson, L.P., Kelly, B.T., McCoy, A.J., Gaffry, T., James, L.C., Collins, B.M., Höning, S., Evans, P.R., and Owen, D.J. (2010). A large-scale conformational change couples membrane recruitment to cargo binding in the AP2 clathrin adaptor complex. Cell **141:** 1220–1229.

Jiang, X., Huang, F., Marusyk, A., and Sorkin, A. (2003). Grb2 regulates internalization of EGF receptors through clathrin-coated pits. Mol. Biol. Cell **14:** 858–870.

Karimi, M., Bleys, A., Vanderhaeghen, R., and Hilson, P. (2007). Building blocks for plant gene assembly. Plant Physiol. **145:** 1183–1191.

Kelly, B.T., McCoy, A.J., Späte, K., Miller, S.E., Evans, P.R., Höning, S., and Owen, D.J. (2008). A structural explanation for the binding of endocytic dileucine motifs by the AP2 complex. Nature **456:** 976–979.

Kitakura, S., Vanneste, S., Robert, S., Löfke, C., Teichmann, T., Tanaka, H., and Friml, J. (2011). Clathrin mediates endocytosis and polar distribution of PIN auxin transporters in *Arabidopsis*. Plant Cell **23:** 1920–1931.

Konopka, C.A., Backues, S.K., and Bednarek, S.Y. (2008). Dynamics of *Arabidopsis* dynamin-related protein 1C and a clathrin light chain at the plasma membrane. Plant Cell **20:** 1363–1380.

Krauss, M., Kukhtina, V., Pechstein, A., and Haucke, V. (2006). Stimulation of phosphatidylinositol kinase type I-mediated phosphatidylinositol (4,5)-bisphosphate synthesis by AP-2μ-cargo complexes. Proc. Natl. Acad. Sci. USA **103:** 11934–11939.

Lee, G.-J., Kim, H., Kang, H., Jang, M., Lee, D.W., Lee, S., and Hwang, I. (2007). EpsinR2 interacts with clathrin, adaptor protein-3, AtVTI12, and phosphatidylinositol-3-phosphate. Implications for EpsinR2 function in protein trafficking in plant cells. Plant Physiol. **143:** 1561–1575.

McMahon, H.T., and Boucrot, E. (2011). Molecular mechanism and physiological functions of clathrin-mediated endocytosis. Nat. Rev. Mol. Cell Biol. **12:** 517–533.

Ortiz-Zapater, E., Soriano-Ortega, E., Marcote, M.J., Ortiz-Masiá, D., and Aniento, F. (2006). Trafficking of the human transferrin receptor in plant cells: Effects of tyrphostin A23 and brefeldin A. Plant J. **48:** 757–770.

Owen, D.J., and Evans, P.R. (1998). A structural explanation for the recognition of tyrosine-based endocytotic signals. Science **282:** 1327–1332.

Page, L.J., and Robinson, M.S. (1995). Targeting signals and subunit interactions in coated vesicle adaptor complexes. J. Cell Biol. **131:** 619–630.

Rappoport, J.Z., and Simon, S.M. (2009). Endocytic trafficking of activated EGFR is AP-2 dependent and occurs through preformed clathrin spots. J. Cell Sci. **122:** 1301–1305.

Robert, S., et al. (2010). ABP1 mediates auxin inhibition of clathrin-dependent endocytosis in *Arabidopsis*. Cell **143:** 111–121.

Robinson, D.G., Hinz, G., and Holstein, S.E.H. (1998). The molecular characterization of transport vesicles. Plant Mol. Biol. **38:** 49–76.

Russinova, E., Borst, J.-W., Kwaaitaal, M., Caño-Delgado, A., Yin, Y., Chory, J., and de Vries, S.C. (2004). Heterodimerization and endocytosis of *Arabidopsis* brassinosteroid receptors BRI1 and AtSERK3 (BAK1). Plant Cell **16:** 3216–3229.

Sauer, M., Balla, J., Luschnig, C., Wiśniewska, J., Reinöhl, V., Friml, J., and Benková, E. (2006). Canalization of auxin flow by Aux/IAA-ARF-dependent feedback regulation of PIN polarity. Genes Dev. **20:** 2902–2911.

Sharfman, M., Bar, M., Ehrlich, M., Schuster, S., Melech-Bonfil, S., Ezer, R., Sessa, G., and Avni, A. (2011). Endosomal signaling of the tomato leucine-rich repeat receptor-like protein LeEix2. Plant J. **68:** 413–423.

Song, K., Jang, M., Kim, S.Y., Lee, G., Lee, G.-J., Kim, D.H., Lee, Y., Cho, W., and Hwang, I. (2012). An A/ENTH domain-containing protein functions as an adaptor for clathrin-coated vesicles on the growing cell plate in Arabidopsis root cells. Plant Physiol. **159:** 1013–1025.

Sun, Y., et al. (2010). Integration of brassinosteroid signal transduction with the transcription network for plant growth regulation in *Arabidopsis*. Dev. Cell **19:** 765–777.

Takano, J., Tanaka, M., Toyoda, A., Miwa, K., Kasai, K., Fuji, K., Onouchi, H., Naito, S., and Fujiwara, T. (2010). Polar localization and degradation of *Arabidopsis* boron transporters through distinct trafficking pathways. Proc. Natl. Acad. Sci. USA **107:** 5220–5225.

Teh, O.-K., Shimono, Y., Shirakawa, M., Fukao, Y., Tamura, K., Shimada, T., and Hara-Nishimura, I. (2013). The AP-1 μ adaptin is required for KNOLLE localization at the cell plate to mediate cytokinesis in *Arabidopsis*. Plant Cell Physiol. **54:** 838–847.

Traub, L.M. (2009). Tickets to ride: Selecting cargo for clathrin-regulated internalization. Nat. Rev. Mol. Cell Biol. **10:** 583–596.

Van Damme, D., Gadeyne, A., Vanstraelen, M., Inzé, D., Van Montagu, M.C.E., De Jaeger, G., Russinova, E., and Geelen, D. (2011). Adaptin-like protein TPLATE and clathrin recruitment during plant somatic cytokinesis occurs via two distinct pathways. Proc. Natl. Acad. Sci. USA **108:** 615–620.

Van Leene, J., Witters, E., Inzé, D., and De Jaeger, G. (2008). Boosting tandem affinity purification of plant protein complexes. Trends Plant Sci. **13:** 517–520.

Van Leene, J., et al. (2010). Targeted interactomics reveals a complex core cell cycle machinery in *Arabidopsis thaliana*. Mol. Syst. Biol. **6:** 397.

Van Leene, J., et al. (2007). A tandem affinity purification-based technology platform to study the cell cycle interactome in *Arabidopsis thaliana*. Mol. Cell. Proteomics **6:** 1226–1238.

Wu, G., Wang, X., Li, X., Kamiya, Y., Otegui, M.S., and Chory, J. (2011). Methylation of a phosphatase specifies dephosphorylation and degradation of activated brassinosteroid receptors. Sci. Signal. **4:** ra29.

Yin, Y., Wang, Z.Y., Mora-Garcia, S., Li, J., Yoshida, S., Asami, T., and Chory, J. (2002). BES1 accumulates in the nucleus in response to brassinosteroids to regulate gene expression and promote stem elongation. Cell **109:** 181–191.

Yu, X., Li, L., Zola, J., Aluru, M., Ye, H., Foudree, A., Guo, H., Anderson, S., Aluru, S., Liu, P., Rodermel, S., and Yin, Y. (2011). A brassinosteroid transcriptional network revealed by genome-wide identification of BESI target genes in *Arabidopsis thaliana*. Plant J. **65:** 634–646.

Wang, Z.Y., Seto, H., Fujioka, S., Yoshida, S., and Chory, J. (2001). BRI1 is a critical component of a plasma-membrane receptor for plant steroids. Nature **410:** 380–383.

Zwiewka, M., Feraru, E., Möller, B., Hwang, I., Feraru, M.I., Kleine-Vehn, J., Weijers, D., and Friml, J. (2011). The AP-3 adaptor complex is required for vacuolar function in *Arabidopsis*. Cell Res. **21:** 1711–1722.